J Mater Sci (2011) 46:7344–7355
DOI 10.1007/s10853-011-5696-0

Production of cellulose nanocrystals using hydrobromic acid and click reactions on their surface

Hasan Sadeghifar · Ilari Filpponen · Sarah P. Clarke · Dermot F. Brougham · Dimitris S. Argyropoulos

Received: 20 April 2011 / Accepted: 4 June 2011 / Published online: 22 June 2011

Abstract Cellulose nanocrystals (CNCs) were prepared by acidic hydrolysis of cotton fibers (Whatman #1 filter paper). In our efforts to select conditions in which the hydrolysis media does not install labile protons on the cellulose crystals, a mineral acid other than sulfuric acid (H_2SO_4) was used. Furthermore, in our attempts to increase the yields of nanocrystals ultrasonic energy was applied during the hydrolysis reaction. The primary objective was to develop hydrolysis reaction conditions for the optimum and reproducible CNC production. As such, the use of hydrobromic acid (HBr) with the application of sonication as a function of concentration (1.5–4.0 M), temperature (80–100 °C), and time (1–4 h) was examined. Applying sonic energy during the reaction was found to have significant positive effects as far as reproducible high yields are concerned. Overall, the combination of 2.5 M HBr, 100 °C, and 3 h associated with the sonication during the reaction generated the highest nanocrystal yields. In addition to the optimization study three types of surface modifications including TEMPO-mediated oxidation, alkynation, and azidation were used to prepare surface-activated, reactive CNCs. Subsequently, click chemistry was employed for bringing together the modified nanocrystalline materials in a unique regularly packed arrangement demonstrating a degree of molecular control for creating these structures at the nano level.

H. Sadeghifar · D. S. Argyropoulos
Organic Chemistry of Wood Components Laboratory, Department of Forest Biomaterials, North Carolina State University, Raleigh, NC 27695-8005, USA

D. S. Argyropoulos (✉)
Department of Chemistry, University of Helsinki, PO Box 55, 00014 Helsinki, Finland
e-mail: dsargyro@ncsu.edu

I. Filpponen
Department of Forest Products Technology, School of Science and Technology, Aalto University, PO Box 16300, 00076 Aalto, Finland

S. P. Clarke · D. F. Brougham
National Institute for Cellular Biotechnology, School of Chemical Sciences, Dublin City University, Glasnevin, Dublin, Ireland

Introduction

Perhaps the earliest technical work on microcrystalline cellulose, or MCC, was documented in a journal article by Battista in 1949 [1]. Battista exposed native and regenerated cellulose to hydrochloric acid, measuring the degree of polymerization of the polymer at different points in time. A decrease in degree of polymerization was observed, but the decrease leveled off after approximately 5 h. Battista proposed that this was evidence to two separate amorphous and crystalline regions in the cellulose. Since then, a vast amount of research has been conducted into the properties of and the processes producing micro- and nano-sized cellulose crystals.

In 1997, Dong et al. [2] published a paper studying the effects of acid hydrolysis conditions on microcrystalline cellulose size and other properties. They used reaction conditions of 45 °C and 62% sulfuric acid and it was found out that the size of the particles decreased sharply as the reaction time was lengthened. Dong et al., on the other hand, found that the average sizes of the crystalline particles levels off after 1 h reaction having lengths approximately of 175 nm. They concluded that the particle sizes decreased sharply at first as the easily reached glycosidic linkages in the amorphous region of cellulose are broken.

Moreover, after the amorphous region is hydrolyzed, it became significantly more difficult for the acid to reach and break the remaining glycosidic linkages in the crystalline region of cellulose.

Dong et al. also introduced a relationship for the reaction time and particle size distribution. It was found that by increasing the reaction time from 20 min to 4 h the particle size distribution was significantly reduced. The study also established a discrepancy between the particle sizes reported through photon correlation spectroscopy (PCS), and transmission electron microscopy (TEM) paired with image analysis. It was postulated that the light scattering technique used in PCS leads to an overestimated fiber lengths.

Work by Beck-Candanedo et al. [3] supports Dong's hypothesis about average particle size and distribution. As reaction time and acid/pulp ratio were both increased, the average nanocrystal length decreased from 147 to 105 nm. More importantly, the standard deviation in the measured lengths of cellulose nanocrystals (CNCs) decreased from 65 to 36, an almost 50% decrease. In Beck-Candanedo's study, the samples were all ultrasonicated after purification to produce stable colloidal suspensions. The sonicator was used for 7 min at 60% power while the solution was cooled in an ice bath to prevent overheating. In our experiments the pulps were sonicated either at room temperature after the hydrolysis reaction or at 80 and 100 °C during the process.

The modification of cellulose surface plays a central role in the field of sustainable chemistry. By the virtue of their huge abundancy and the structural and superstructural diversity polysaccharides are ideal starting materials for defined modifications and specific applications [4]. The chemical modification of CNCs provides a versatile route for structural and property design of such materials [5]. Due to the chemical functionality of cellulose (bearing hydroxyl and/or carboxylic acid groups), esterification and etherification are the most common approaches for modification reactions of polysaccharides. Moreover, oxidation and homogeneous nucleophilic substitution reactions are applied but to a lesser extent. However, these reactions often need organic solvents and/or rather harsh reaction conditions to be sufficient enough. Therefore, new methods for the biomaterial functionalizations are nowadays heavily explored. Click chemistry is one of the most promising approaches up to date and increasing amount of research efforts are conducted for the 'click'-based modifications of biomaterials [6–8]. The reactions are experimentally simple needing no protection from oxygen, requiring only stoichiometric amounts of starting materials, and generating virtually no by-products. The wide scope, high selectivity, mild reaction conditions, and nearly quantitative yields of these conversions ideally comply with our needs for rapid, selective and specific chemistry on polysaccharides which possess multifunctional and multichiral centers. The 1,3-dipolar cycloaddition of an azide moiety and a triple bond (Huisgen reaction) has rapidly become the most popular click reaction to date [9, 10].

In this effort, we confirmed previous reports that showed positive effects of sonic energy being applied after the acidic hydrolysis. Furthermore, we extended our measurements and showed that the yields of nanocrystals can dramatically be increased if the ultrasonic treatment (2.5 M HBr, 80 °C, 3 h) was applied during the hydrolysis increasing the yields from 35 to 60%. In addition, three important CNC derivatives including TEMPO-oxidized CNCs as well as alkyne and azide-bearing CNCs were prepared. Finally, the alkyne and azide surface functionalized CNC precursors were brought together via click chemistry, creating a unique nanoplatelet material as evidenced by detailed TEM investigations.

Materials and methods

Materials

Whatman #1 filter paper was used as a starting material for the CNCs production. HBr and NaOH, TEMPO and Acetamino-Tempo-radical, sodium bromide, NaClO and other materials were purchased from Sigma-Aldrich.

Formation of cellulose nanocrystals (CNCs)

The CNCs were formed by acidic hydrolysis similar to the procedure used by Araki et al. [11–13] as illustrated in Scheme 1. A typical procedure was as follows. 2.0 g of cellulose pulp obtained from Whatman #1 filter paper (98% α-cellulose, 80% crystallinity) was blended by a 10 Speed Osterizer® Blender. The resulting pulp was hydrolyzed with 100 mL of 1.5, 2.5, or 4.0 M HBr at 100 °C for 1, 2, 3, or 4 h. The ultrasonication was applied either during (every 60 min) or after the reaction at the room temperature (Omni-Ruptor 250 W ultrasonic homogenizer, 50% power, 5 min). The resulting mixture was diluted with de-ionized (D.I.) water followed by five cycles of centrifugation at 1,500×*g* for 10 min (IEC Centra-CL3 Series) to remove excess acid and water soluble fragments. The fine cellulose particles became dispersed in the aqueous solution approximately at pH 4. The turbid supernatant containing the polydisperse cellulose particles was then collected for further centrifugation at 15,000×*g* for 45 min (Automatic Servall® Superspeed Centrifuge) to remove ultra-fine particles. Ultra-fine particles with small aspect ratio were removed from the upper layer, and the precipitation (after the high-speed centrifugation) was dried using a lyophilizing system (Labconco, Kansas City, MU).

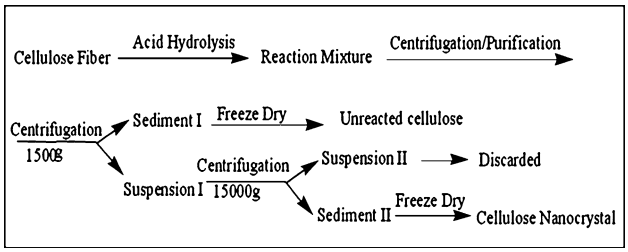

Scheme 1 Schematic representation of the preparation of cellulose nanocrystals (CNCs)

Grafting on the reducing end groups of CNCs

Reducing end groups of CNC were blocked according to Sipahi-Saglam et al. [14]. 1 g (6.2 mmol) of micro-crystalline cellulose was suspended in 20 mL borate buffer (0.2 N boric acid) and 0.216 g (2 mmol) of phenylhydrazine was added. The flask was closed and shaken in an oil bath tempered to 35 °C for 72 h. At the completion of reaction time the product was centrifuged, washed twice with 100 mL tetrahydrofuran and five times with D.I. water. The purification was completed with the dialysis of the modified cellulose (CNC-PH) against D.I. water for 3 days. The ^{1}H NMR of acetylated sample showed an aromatic peak at around 7 ppm (Fig. 1).

TEMPO-mediated oxidation of CNCs in alkaline conditions

TEMPO-oxidized CNCs were synthesized according to the literature methods [15]. 648 mg (4 mmol of glucosyl units) of CNCs were suspended in water (50 mL) containing 10 mg of 2,2,6,6-tetramethyl-1-piperidinyloxy (TEMPO, 0.065 mmol) and 200 mg of sodium bromide (1.9 mmol) at room temperature for 30 min. The TEMPO-mediated oxidation of the CNCs was initiated by slowly adding 4.90 mL of 13% NaClO (8.6 mmol) over 20 min at room temperature under gentle agitation. The reaction pH was monitored using a pH meter and maintained at 10 by incrementally adding 0.5 M NaOH. When no more decrease in pH was observed, the reaction was considered complete. About 5 mL of methanol was then added to react and quench with the extra oxidant. After adjusting the pH to 7 by adding 0.5 M HCl, the TEMPO-oxidized product was washed with D.I. water by centrifugation and further purified by dialysis against D.I. water for 2 days. 550 mg of solid was recovered after freeze-drying. FTIR measurements showed a carboxylic acid peak at 1730 cm^{-1} (Scheme 2(b)).

Acetamino-TEMPO-mediated oxidation of CNCs in neutral conditions

Acetamino-TEMPO-oxidized CNCs were synthesized according to the procedure by Saito et al. [16]. 648 mg

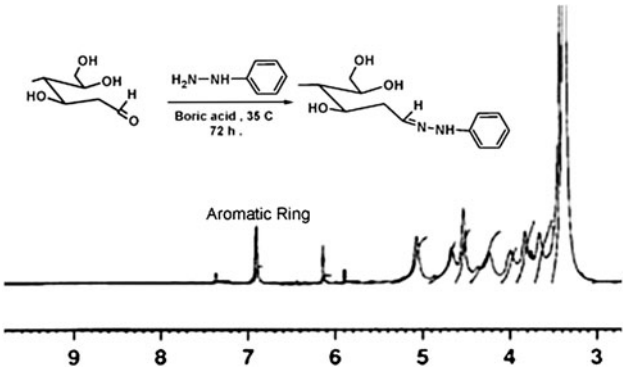

Fig. 1 ^{1}H NMR spectrum of reducing end-blocked CNCs

(4 mmol of glucosyl units) of CNCs were suspended in 65 mL of 0.1 M acetate buffer (pH 5.8) containing $NaClO_2$ (80%, 0.55 g, 4.8 mmol) and 4-acetamide-TEMPO (0.06 g, 0.29 mmol) and placed in an Erlenmeyer flask equipped with a magnetic stirrer. Next, diluted NaClO solution (0.2 mL, 0.32 mmol) was added at one step to the suspension. The flask was capped and the mixture was stirred at 40 °C for 1 day. Then $NaClO_2$ (0.55 g, 4.8 mmol) and NaClO (0.2 mL, 0.32 mmol), were added at one step to the flask, and the mixture was stirred at 40 °C for additional 2 days. Finally, the oxidation was quenched by adding an excess of ethanol. The precipitates formed after ethanol addition were collected and washed two times with 80% aqueous ethanol with centrifugation. The oxidized product was dispersed in D.I. H_2O, dialyzed 3 days against D.I. H_2O followed by centrifugation to prepare more concentrated suspensions.

Synthesis of alkyne-bearing CNC-derivative (CNC-PR)

Never dried TEMPO-oxidized CNCs (100 mg) were mixed in 15 mL of MES buffer (50 mM, pH 4). In typical synthesis, 250 mg of EDC·HCl [*N*-(3-dimethylaminopropyl)-*N*′-ethylcarbodiimide hydrochloride)], 150 mg of NHS (*N*-hydroxysuccinimide), and 200 μL of propargylamine, respectively, were added to the CNC suspension [17]. The reaction was performed at room temperature under stirring for 24 h. The resulting mixture was dialyzed (cutoff = 12 kDa) against a saturated NaCl solution for 1 day and then against distilled water for 3 days. Finally, the CNC-PR derivative (Scheme 2(b)) was recovered and kept in water suspension. Small amount of product was freeze-dried for the elemental analysis. The degree of substitution (DS = 0.073) was calculated according to the elemental analysis results (C 41.58%, H 6.65%, O 51.14%, N 0.63%).

Synthesis of azide-bearing CNC-derivative (CNC-AZ)

The primary hydroxyl groups on the surface of oxidized CNCs were tosylated according to the literature with some

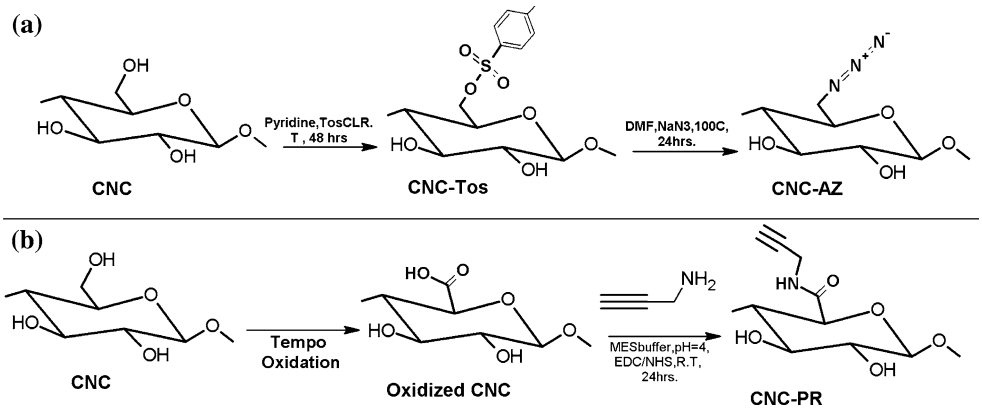

Scheme 2 Schematic representation for the synthesis of CNC-AZ (**a**) and CNC-PR (**b**)

modifications [18–20]. 0.5 g of CNCs (3.1 mmol of glucosyl units) were suspended in pyridine (10 mL), and the mixture was cooled down to 10 °C. Next, tosyl chloride (0.9 g, 5 mmol) was added and the reaction mixture was stirred for 2 days in room temperature. The product was isolated by adding 100 mL of ethanol and the resulting precipitate was collected by filtration. Precipitate was washed five times with ethanol (50 mL) and five times with D.I. H_2O (50 mL) and finally freeze-dried. Tosylated CNCs (CNC-Tos) were suspended in 20 mL of DMF (400 mg) followed by the careful addition of sodium azide (400 mg). The reaction mixture was stirred at 100 °C for 24 h and then precipitated by adding 50 mL of D.I. H_2O. Precipitate was washed five times with ethanol (50 mL) and five times with D.I. H_2O (50 mL) followed by the dialysis against D.I. H_2O for 3 days. Finally, the CNC-AZ derivative was recovered and kept in water suspension (Scheme 2(a)). Small amount of product was freeze-dried for the elemental analysis. The degree of substitution (DS = 0.15) was calculated according to the elemental analysis results (C 41.06%, H 6.35%, O 48.84%, N 3.75%).

Synthesis of "click"-product (CNC-click) in DMF

50 mg amounts of never dried CNC-AZ and CNC-PR were mixed in 5.0 mL of distilled DMF. Next, a mixture of 7 mg $CuBr_2$, 20 mg of ascorbic acid, and 50 μL trimethylamine dissolved in 1 mL DMF were added and the mixture was stirred overnight leading to a formation of a stable gel (CNC-Click: Scheme 3). Gel was separated by centrifugation and washed five times with ethanol and three times with water and dialyzed against EDTA solution (10 mM) for 12 h and finally against distilled water for 3 days.

Synthesis of "click"-product (CNC-click) in water

50 mg amounts of CNC-AZ and CNC-PR were mixed in 5.0 mL of distilled water. Next, a mixture of 7 mg $CuSO_4{\cdot}5H_2O$ and 20 mg of ascorbic acid in 1 mL water was added and the mixture was stirred for 3 min leading to a formation of a stable gel (click-gel: Scheme 3). The gel was left at rest overnight and then dialyzed against EDTA solution (10 mM) for 12 h and finally against distilled water for 3 days.

Benzoylation of cellulose and CNCs

Whatman #1 filter paper was homogenized in a Wearing blender in prior to benzoylation. The method described below was developed by the group of Argyropoulos following the principles established in the work described elsewhere [21, 22]. Ionic liquid ([Amim]Cl, 950 mg) was added to cellulose sample (50 mg) in a 15 mL sample bottle, vortexed until all solid particles had dispersed and heated at 80 °C with magnetic stirring until the solution was transparent (2 h). Pyridine (330 μL, 3.7 mmol) was added and the solution was vortexed until visibly homogeneous and allowed to cool down to room temperature. Benzoyl chloride (380 μL, 3.3 mmol) was added in one portion and the resulting mixture was vortexed until the formation of homogeneous white paste. The sample was then heated at 55 °C for 3 h with magnetic stirring and then allowed to cool down to room temperature. The mixture of deionized water (2.5 mL) and EtOH (7.5 mL) was added and the mixture vigorously shaken and vortexed for 5 min. The solid was filtered off through a sintered funnel (grade M), washed further with EtOH and purified with MeOH (stirred overnight without heating overnight). Finally, the resulting solid was filtered off to give white powders. The yields of benzoylated cellulose and CNCs were 100 and 84 mg, respectively. Cellulose benzoates were analyzed by gel permeation chromatography (GPC).

X-ray diffraction

Wide-angle X-ray diffraction (WAXD) measurements were performed with a Siemens type-F X-ray diffractometer using a Ni-filtered Cu K_α radiation source (k = 1.54 Å). The

Scheme 3 Schematic representation of the click reaction between CNC-AZ and CNC-PR (CNC-click product)

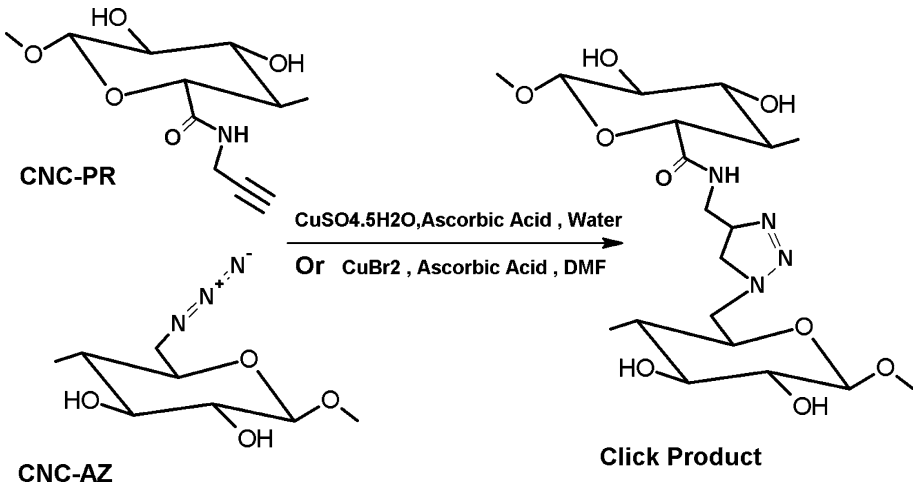

diffraction intensities were measured every 0.1° from $2\theta = 5°$ to 30° at a rate of $2\theta = 3°$/min. The supplied voltage and current were 30 kV and 20 mA, respectively.

Transmission electron microscopy (TEM)

A suspension (0.01% w/v in water) of CNCs was prepared. Drops of suspensions were deposited on carbon-coated electron microscope grids, negatively stained with uranyl acetate and allowed to dry. The grids were observed with a Philips 400T microscope operated at an accelerating voltage of 120 kV.

Gel permeation chromatography (GPC)

GPC measurements were carried out with a Waters GPC 510 pump equipped with UV and RI detectors using THF as the eluent at a flowrate of 0.7 mL/min at room temperature. Two Ultrastyragel linear columns linked in series (Styragel HR 1 and Styragel HR 5E) were used for the measurements. Standard mono-disperse polystyrenes with molecular weight ranges from 0.82 to 1860 kg/mol were used for the calibration. The number- and weight-average molecular weights were calculated using the Millenium-software of Waters.

^{1}H NMR spectroscopy

NMR measurements were acquired using on a Bruker 300 MHz spectrometer equipped with a Quad probe dedicated to ^{31}P, ^{13}C, ^{19}F, and ^{1}H acquisition.

Dynamic light scattering and zeta potential

TEMPO-oxidized CNCs were performed at 25 °C on a NanaZS particle sizer (Malvern Instruments, Malvern, UK) using a detection angle of 173° and a 3 mW He–Ne laser operating at a wavelength of 633 nm. The d_{hyd} (hydrodynamic size) values from dynamic light scattering (DLS) reported are the Z-average diameters (mean hydrodynamic diameter based upon the intensity of scattered light). The polydispersity indices (PDIs) were also calculated from the cumulants analysis as defined in ISO13321.26. Note that the DLS convention is the opposite of that used for conventional polymer polydispersity (PD). PDI values range from 0 to 1; values below 0.35 are consistent with a unimodal size distribution; values below 0.25 are indicative of some control over size; values lower than 0.25 demonstrate increased monodispersity of the distribution. Zeta potential measurements were made using the M3-PALS technique.

Results and discussion

A number of different factors affecting the acidic hydrolysis of cellulose were examined. A complete set of investigated parameters include: reaction time and temperature, the concentration of acid (HBr), and the effect of applied external energy (ultrasonic). The main focus was to optimize the conditions needed for the high yield production of CNCs while retaining the uniform dimensional appearance of produced crystals. In our efforts to increase the yields of nanocrystals the ultrasonic energy was applied on the course of the reaction or after the reaction to break down the aggregates and to further promote the efficiency of acid hydrolysis. While the application of ultrasonic energy after hydrolysis has been previously documented, efforts to apply sonic energy during the acidic hydrolysis have never been undertaken. The ultrasonication device has a tip made of titanium which sets limitations for the type of acid used in the hydrolysis medium. Due to the corrosive nature of HCl toward the titanium tip of the sonic gun, our sonication hydrolysis experiments were carried out in HBr solutions (inert towards titanium).

Due to the cellulose's strong ability to form hydrogen bonds, the produced nanocrystals tended to agglomerate to form larger particles. Instead of being removed as part of the suspension after centrifugation, these aggregated particles precipitated at the bottom of the centrifugal tube and were discarded as sediment. This significantly decreased the yield of CNCs from the hydrolysis reaction. The aggregate formation manifested itself especially in the absence of surface charges when the repulsion forces between the individual nanocrystals were minimized. One solution for decreasing the aggregation issue is to introduce negative charges on the surface of CNCs. Sulfuric acid is known to introduce negative charges on the surface of the CNCs via an esterification reaction with the sulfate anions [3, 11, 23]. While such charges may be of some benefit in stabilizing nanocrystal suspensions in the study of their chiral nematic properties, such groups create labile centers and sites of potential side reactions during subsequent site-specific grafting. Therefore, to benefit our ultimate objectives aimed to site-specific modification of CNCs we decided to use HBr for the acidic hydrolysis of cellulose to avoid possible side reactions. Moreover, elemental analysis on well-washed nanocrystals prepared under HBr hydrolysis conditions showed the complete absence of bromine indicative of the lack of side reactions. It is also well known fact that HBr is a stronger acid than HCl or H_2SO_4 which can offer further savings in chemical use when a large scale manufacture of CNCs is considered.

The effect of acid concentration, reaction temperature, and reaction time to the yield of CNCs

Reaction time, reaction temperature, and HBr concentration are the parameters that will effect on the efficiency of acid hydrolysis. It is expected that the reaction time and temperature will have a significant impact to the achieved yields as the heterogeneous diffusion of the acid to the amorphous regions of cellulose does not occur instantaneously. Furthermore, the relative rate of the hydrolysis will be faster in the beginning of the process when the easily accessible amorphous regions are being hydrolyzed and later slow down significantly as the acid attacks the reducing end and the surface of the residual crystalline regions. It is important to note here that the starting material is known to have 80% crystallinity (Whatman #1) thus containing 20% of more easily hydrolysable amorphous cellulose. Therefore, the maximum yield of highly crystalline CNCs is 80% from the starting weight of dry cellulose pulp. In practice, the yields are expected to be lower as small parts of the crystalline regions will be hydrolyzed as well. Nevertheless, the hydrolysis conditions should be mild enough to avoid complete hydrolysis of cellulose to glucose or even carbonization.

Figure 2 demonstrates the effects of reaction time and temperature to the yield of CNCs during the hydrolysis with 2.5 M HBr. It can be seen that in both selected hydrolysis temperatures, 80 and 100 °C, the yields are increasing along the hydrolysis time. The highest yield, 70% from the starting material, was achieved from the hydrolysis reaction of 3 h at 100 °C (Fig. 2b). It is worth to mention here that 70% yield is very close to theoretical maximum of 80% as mentioned above. At this point it can be stated that the 30% loss of material corresponds well with the amount of less ordered amorphous cellulose in starting material. Moreover, the results pointed out the positive effects of the applied ultrasonication which will be discussed later in this manuscript.

Figure 3 compares the yields of CNCs in relation to the acid concentration used in the hydrolysis reaction. It can clearly be seen that the yields are significantly higher when the HBr concentration is increased from 1.5 to 2.5 M. However, further increase in concentration up to 4.0 M did not improve the yields notably. It is also worth mentioning here that the CNCs collected after the 4.0 M HBr treatment appeared darker in color than the ones from milder hydrolysis treatments. This can be indicative from the side reactions, such as dehydration, that are known to occur under harsh reaction conditions.

The effect of ultrasonication to the yield of CNCs

We anticipate that the application of sonic energy may significantly affect the production of CNCs. This is because using sonic energy during hydrolysis may disrupt agglomerated particles when the pulp is still reacting with the HBr. This should affect the yield data by increasing the area of the pulp exposed to acid hydrolysis. The effect of ultrasonic irradiation on the property and yield of CNCs was examined by applying ultrasonication during or after the acidic hydrolysis. Typically, a 5 min 50% power (125 W) ultrasound treatment was applied either after the hydrolysis reaction or in 5 min segments every 60 min during the hydrolysis reaction.

The nanocrystal yields shown in Table 1 indicate that the amount of CNCs (Sediment II, see Scheme 1) is increased at the expense of unreacted cellulose (Sediment I, see Scheme 1) due to the fact that the ultrasonic energy is able to disrupt possible nanocrystal aggregation more efficiently when it is applied during hydrolysis rather that after hydrolysis. It is also important to note that the total final yields were constant ranging from 83 to 85% for all conditions examined. These similar total yields imply that the ultrasonic energy applied during hydrolysis caused no irreversible chemical bond scission within the nanocrystals.

Furthermore, the effect of the applied ultrasonication after or during the hydrolysis reaction was compared.

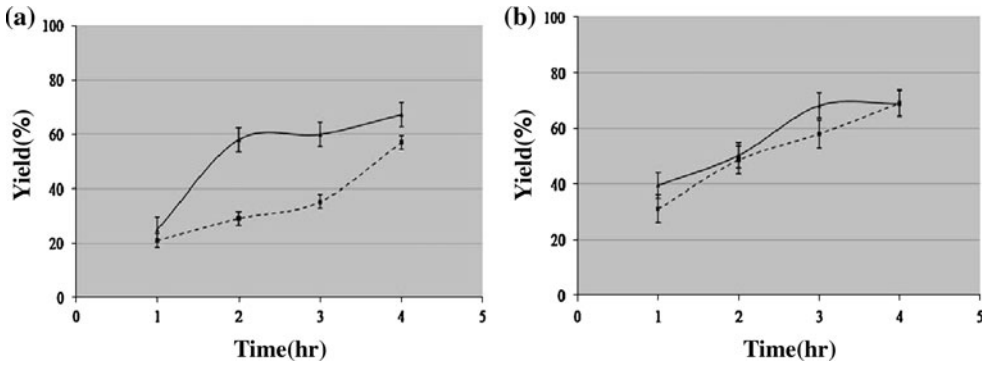

Fig. 2 **a** The effect of the applied ultrasonication to the yields of cellulose nanocrystals from the hydrolysis with 2.5 M HBr at 80 °C and **b** hydrolysis with 2.5 M HBr at 100 °C (*solid line* ultrasonication during the reaction, *dashed line* ultrasonication after the reaction)

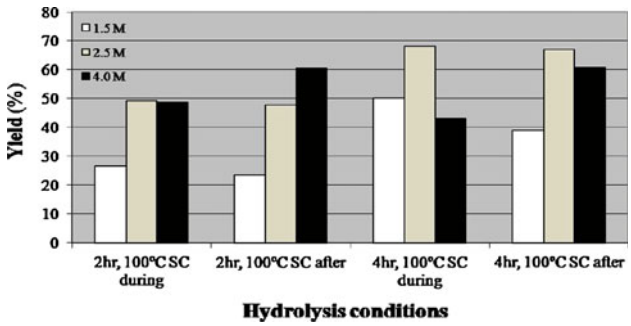

Fig. 3 The yields of cellulose nanocrystals with different acid (HBr) concentrations

Figure 2 shows the CNC yields achieved from the hydrolysis conditions of 2.5 M HBr at 80 and 100 °C as a function of hydrolysis time comparing the moment of applied ultrasonication (during vs. after). It can be seen that at higher reaction temperature (100 °C) the moment of ultrasonication has practically no effect on the yields of CNCs (Fig. 2b). However, at a lower temperature (80 °C) the effect is more pronounced, i.e., ultrasonication during the hydrolysis reaction gave significantly higher CNC yields especially at shorter reaction times (2 and 3 h). The difference could be explained with the total amount of energy put in the hydrolysis system. At higher hydrolysis temperatures the additional energy from the ultrasonication during the hydrolysis reaction does not benefit the formation of CNCs as much as at lower hydrolysis temperatures.

X-ray diffraction experiments

As anticipated, the CNCs obtained after acid hydrolysis were highly crystalline structures as shown by the X-ray diffraction data in Fig. 4. Proper control of the hydrolysis conditions resulted in the selective degradation and preferential removal of the amorphous cellulosic fraction. The crystallinities were calculated according to Segal et al. (Eq. 1) [24]. It was found out that crystallinity index increased from 80 to 91% during the acidic hydrolysis process.

$$\text{Cr.I.}\,(\%) = ((I_{002} - I_{\text{am}})/I_{002}) \times 100 \quad (1)$$

where I_{002} is the maximum intensity from (002) plane at $2\theta = 22.8°$ and I_{am} is the intensity of the background scatter measured at $2\theta = 18°$.

Morphological characterization—transmission electron microscopy (TEM)

The length distribution of CNCs was estimated from TEM images. TEM data demonstrates that at this point in our work we are able to develop rod-like nanocrystals of approximately 100–200 nm (Fig. 5a). Yet, the aggregation of cellulose whiskers hindered the determination of transverse dimensions. However, the average crystallite sizes can be obtained from the X-ray diffraction data by using the Debye–Scherrer formula (Eq. 2) [25]. The results from X-ray diffraction and TEM are summarized in Table 2.

$$D = k\,\lambda\text{Cu}/\beta\cos\theta \quad (2)$$

Table 1 Comparison of yields with/without ultrasonication applied during the hydrolysis of cellulose

Reaction time	2 h	2 h-U	4 h	4 h-U
Cellulose nanocrystals (Sediment II)[a]	23.5%	26.6%	39.0%	50.1%
Unreacted cellulose (Sediment I)[a]	61.8%	58.8%	45.1%	32.7%
Total	85.3%	85.4%	84.1%	82.8%

Hydrolysis in 1.5 M HBr at 100 °C 2 h or 4 h

U—5 min ultrasonication applied every 60 min during acid hydrolysis

[a] For precise definition of these terms see Scheme 1

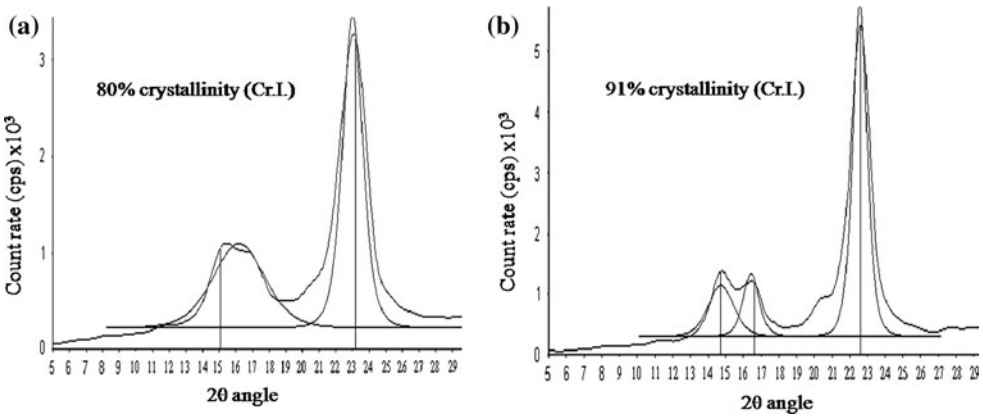

Fig. 4 X-ray diffraction of cellulose powder (Whatman #1) (**a**) and cellulose nanocrystals (**b**)

here $k = 0.9$, $\lambda Cu = 0.154056$ nm, $\beta = FWHM$ (full width at half maximum, or half-width) in radians, $\theta =$ the position of the maximum of diffraction.

The prepared cotton CNCs has a rectangular shape with average dimensions of 8.6 × 7.7 nm (Table 2). Thus, the amount of individual cellulose chains within a cotton crystallite can be calculated using the two lattice parameters of cellulose I_β unit cell, $a = 0.504$ nm and $b = 0.62$ nm, respectively [26, 27]. Based on this model, the planes (1 −1 0) corresponding to 0.61 nm are parallel to the long side of the rectangular nanocellulose section whereas the 0.54 nm (1 1 0) are parallel to the short side [28, 29]. Thus within this average crystal, there are $(8.6 \times 7.7)/(0.61 \times 0.54) = 201$ cellulose chains. At the surface, there are $2 \times (8.6/0.54) + 2 \times (7.7/0.61) = 57$ surface chains. The ratio of surface chains to the total number of chains within the crystals is therefore of 0.29. If we now consider the accessible hydroxymethyl groups, only half of these are available, the other being buried inside the crystalline whisker as a consequence of the two fold screw axis of the cellulose chain. Thus, the maximum degree of primary hydroxyl groups in the surface of CNCs is about 0.29/2 = 0.145.

Molecular weight distribution of CNCs

By the virtue of the hydrophobic benzoyl groups introduced during the successful benzoylation reactions cellulose samples became soluble in THF which in turn made it possible to determine the molecular weight of cellulosic samples by using GPC. The GPC chromatograms for the starting material cellulose and CNCs are shown in Fig. 6. It is obvious that the CNCs are of a lower molecular weight than the starting material cellulose due to the hydrolysis of the amorphous regions of the starting cellulose. In fact, the molecular weight of cellulose dropped from 95×10^3 to

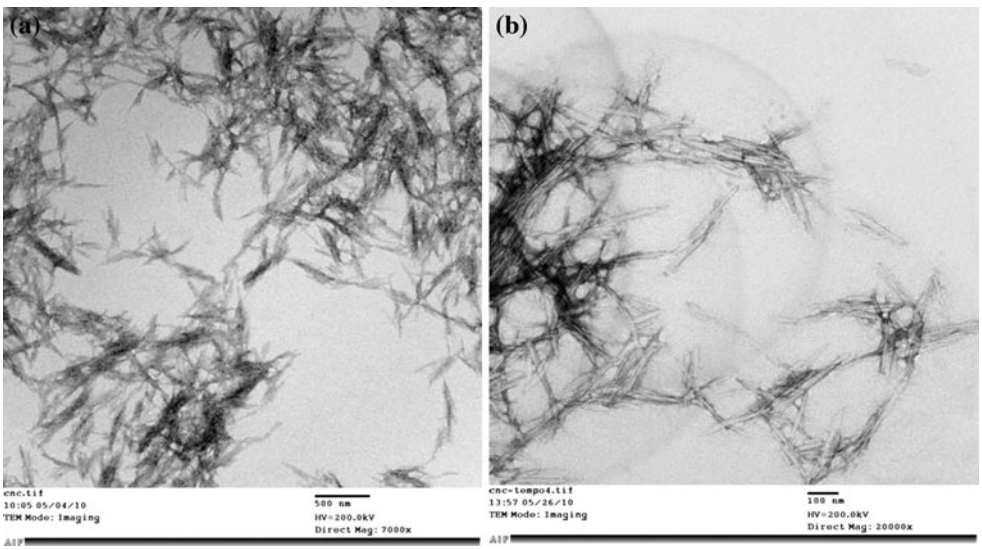

Fig. 5 **a** TEM image of cellulose nanocrystals (100 °C, 3 h, ultrasonication during the hydrolysis reaction) and **b** TEM image of acetamino-TEMPO-oxidized cellulose nanocrystals

Table 2 Crystallinity and average sizes of cellulose nanocrystals determined by XRD and TEM

Sample	Crystallinity index (Cr.I.)	Transverse 1 (nm)	Transverse 2 (nm)	Length (nm)
100 °C, 1 h-U	88	7.0	7.6	100–400
100 °C, 2 h-U	89	7.6	7.7	100–400
100 °C, 3 h-U	91	8.6	7.7	100–400

U—5 min ultrasonication applied every 60 min during acid hydrolysis

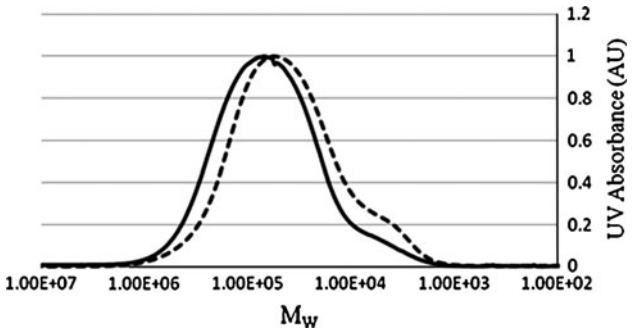

Fig. 6 GPC chromatogram of benzoylated cellulose (Whatman #1, *solid line*) and benzoylated cellulose nanocrystal (*dashed line*)

Table 3 Molecular weight distributions of starting material cellulose (Whatman #1) and cellulose nanocrystals

Sample	Mw (1×10^3 g mol^{-1})	Polydispersity (PD)
Whatman #1	95	3.8
Cellulose nanocrystals	69	4.1

69×10^3 g mol^{-1} during the acidic hydrolysis resulting in CNCs with somewhat increased polydispersity (Mw/Mn, Table 3).

TEMPO-oxidation of CNCs

TEMPO-oxidation selectively oxidizes the primary hydroxyl groups while leaving unaffected the secondary hydroxyl groups [30]. Two separate methods for the TEMPO-assisted oxidation were investigated. Based on the arrangement of the cellulose molecule in the crystalline unit cell [31]. The carboxylic groups created on the nanocrystal surface should be 1.0 nm apart in the longitudinal direction and 0.8 nm apart in the width direction. This is a unique feature of CNCs. FTIR spectra of TEMPO and acetamino-TEMPO-oxidized CNCs show a new band at around 1730 cm^{-1} when compared to the starting CNCs. The carboxyl content of oxidized cellulose samples was determined by acid–base titrations as described elsewhere [15]. It was found out that 15.4% of total hydroxyl groups of CNCs were converted to carboxylic acid groups by using acetamino-TEMPO-mediated oxidation. In the case of TEMPO-mediated oxidation the degree of oxidation (DO) was found to be 13.4%. At this point it can be concluded that the achieved DO values are in a good agreement with the calculated theoretical maximum degree (14.5%) of the primary hydroxyl groups in the surface of CNCs.

The fact that CNCs have the innate capacity to form hydrogen bonds creates systems that may readily aggregate which can present serious characterization problems especially when examined under scanning electron microscopy (SEM). However, oxidation of the surface hydroxyl groups of CNCs will increase its dispersability by introducing negative charges on the surface (Fig. 5b) [32, 33]. It was found out that the acetamino-TEMPO-oxidized CNCs (DO = 0.154) form aqueous colloidal suspensions with moderately high zeta potential values (−30 mV) that explains the increased stability of the suspensions (Table 4). The suspensions were formed of relatively monodisperse agglomerates of CNCs with d_{hyd} value of 190 nm (Table 4). However, attempts for determining the iso-electric point failed because of the rapid aggregation at pH < 5.8. It is also important to note here that the zeta potential had already increased to −19 mV at pH 5.8.

TEMPO-oxidized CNCs (DO = 0.134), form suspensions consisting of aggregates with similar average hydrodynamic size than that of CNC produced by acetamino-TEMPO-mediated oxidation. However, these suspensions were found to be less stable and significantly more polydisperse, i.e., reduced surface charge and higher PDI (Table 4). Furthermore, the zeta potential measurements revealed surprisingly low values for TEMPO-oxidized CNCs which can be explained, at least partly, with the larger size distribution of TEMPO-oxidized CNCs.

Synthesis of CNCs bearing azide groups (CNC-AZ)

Tosylation is the first step for the synthesis of azido-modified cellulose [18]. FTIR spectrum of tosylated cellulose (Fig. 7(a)) shows the typical absorption bands of the cellulose backbone as well as the signals for the aromatic rings of tosylates at 1598, 1495, and 815 cm^{-1}, respectively. Furthermore, two strong stretching bands at 1359 and 1175 cm^{-1} (t SO2) confirmed the presence of the tosyl groups. It should be mentioned here that instead of dissolving CNCs in ionic liquid the tosylation reaction was

Table 4 Colloidal analysis of aqueous cellulose nanocrystal suspensions by light scattering

Sample	d_{hyd} (nm)/PDI	Zeta potential (mV)	Stability
Acetamino-TEMPO-ox. CNC (DO 0.154)	190/0.17	-30 ± 5 (at pH 6.8)	$5.8 < pH < 8$ and >1 week at pH 6.8
TEMPO-ox. CNC (DO 0.134)	191–233/0.30–0.36	-1 ± 5	<1 week at pH 6.8

performed in pyridine suspensions of CNCs to modify only the surface hydroxyl groups of CNCs. This is important especially when retaining the crystalline form of CNCs is considered. In the next step, tosyl groups were transformed to azido groups by a homogeneous nucleophilic displacement reaction with sodium azide using DMF as a solvent (Scheme 2). The FTIR spectrum of azide-modified CNCs showed a new stretching band for the azide moiety at 2113 cm^{-1} while the aromatic bands of the tosyl groups at 1598, 1500, and 1453 cm^{-1} were disappeared (Fig. 7(a)). Moreover, the elemental analysis of CNC-AZ showed nitrogen content of 3.75% corresponding to the DS value of 0.14. When this value is compared to the theoretical maximum value of the surface hydroxyl groups (14.5%) it is apparent that almost all the primary hydroxyl groups on the surface of CNCs were converted to azido groups.

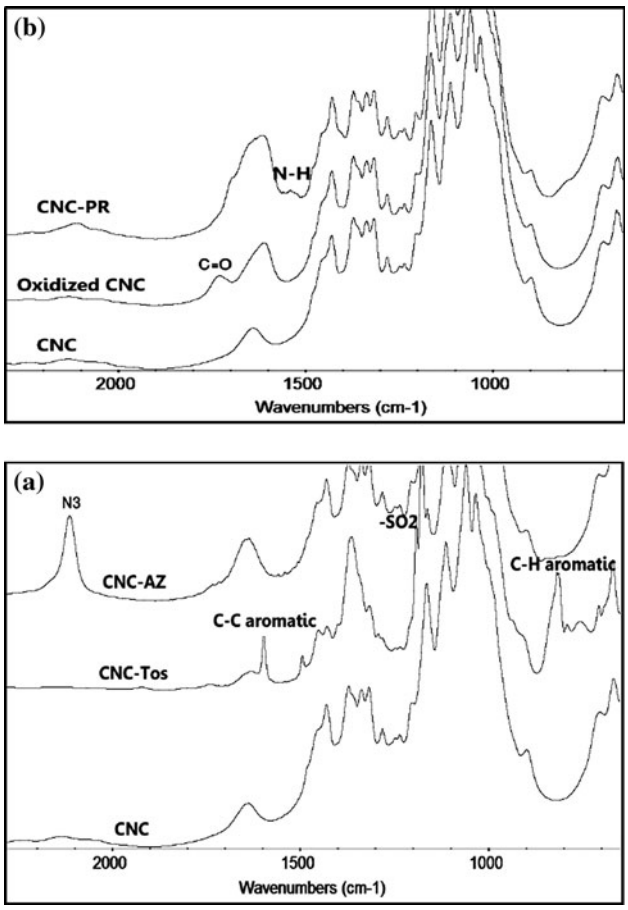

Fig. 7 FTIR spectra of azide-modified (**a**) and alkyne-modified (**b**) cellulose nanocrystals

Synthesis of CNCs bearing alkyne groups (CNC-PR)

The reaction of acetamino TEMPO-oxidized CNCs with propargylamine was monitored by FTIR and elemental analysis (nitrogen content). Figure 7(b) clearly displays the carbonyl stretching band at 1730 cm^{-1} for the TEMPO-oxidized CNCs. This band is seen to be eliminated during the formation of the alkyne derivative (CNC-PR, Fig. 7(b)). The disappearance of the carbonyl stretching band is due to the formation of the amide linkages between the TEMPO-oxidized CNCs and amine-bearing precursor molecules. The amides, on the other hand, are known to have characteristic stretching band at around 1650 cm^{-1} and as such the overlapping with the absorbed water band (1640 cm^{-1}) is unavoidable. However, a new band at 1545 cm^{-1} (N–H) was apparent (Fig. 7(b)). Moreover, the elemental analysis of CNC-PR showed nitrogen content of 0.63% corresponding to the DS value of 0.073. When this value is compared to that obtained for the degree of oxidation (DO = 0.154) it is apparent that approximately half of the primary hydroxyl groups on the surface of CNCs were converted to alkyne groups (DS $\sim$ 50%).

Synthesis of nanoplatelet CNCs (CNC-click)

Our recent findings implied rather regular and mainly vertical linking array of the click chemistry modified CNCs in aqueous suspension [17]. However, a minor degree of linking was found to occur, most likely, via the chain ends of the crystals causing growth in lateral dimension. The observed lateral linking is not totally surprising when one consider the chemistry of the oxidative treatment of the starting CNCs. In addition to oxidizing the surface hydromethyl groups, TEMPO-mediated oxidation may also introduce carboxylic groups to the reducing ends of the CNCs [34–36]. Therefore, the oxidized reducing end groups can become reactive toward the derivatization conditions that were used to form the alkyne and azido bearing click chemistry precursors. Subsequently, the modified reducing end groups can also react under the click chemistry conditions resulting in the multi-dimensional but rather regular growth in the CNC network.

To further elucidate the role of the reducing end aldehyde groups, a set of nanocrystals with chemically blocked reducing end groups was prepared. In detail, the reducing end groups in CNCs were blocked by phenylhydrazine via

hydrazone linkages as anchor groups [14]. Subsequently, a small batch of the reducing end derivatized CNCs was acetylated to make the material soluble in DMSO that allowed for the ^{1}H NMR analysis of the product. ^{1}H NMR spectrum of the grafted CNCs revealed signals in aromatic region of the NMR (~7.0 ppm) thus pointing toward a successful grafting reaction. These reducing end-blocked CNCs were used further for the derivatization reactions (TEMPO-oxidation, azidation/alkynation, click reaction). The formation of the cross-linked CNCs (CNC-click) via click chemistry reaction is shown in Scheme 3. Click reactions were carried out in both aqueous and organic media with the aim of evaluating the role of the self-assembly forces that may operate between the individual hydrated functionalized click precursor nanocrystals [37, 38] Once brought at close proximity by the hydration forces CNCs are locked into place via the reaction between azide and the alkyne moieties.

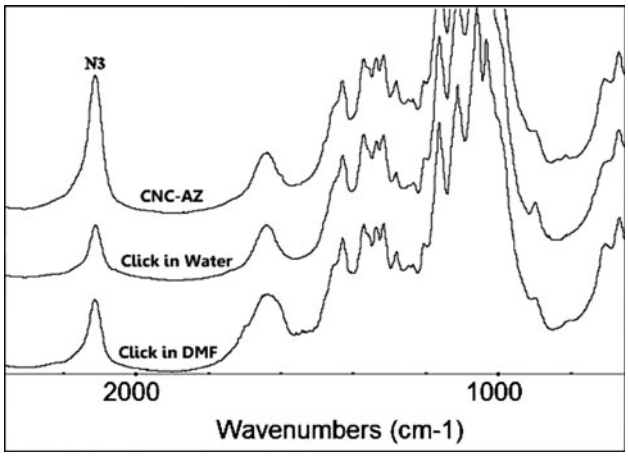

Fig. 8 FTIR spectra of CNC-click product prepared in water and DMF

It can clearly be seen from the FTIR spectra in Fig. 8 that after the click reaction the intensities of the characteristic azide stretching bands decreased approximately 50% when compared to the intensity of the azide stretching band in CNC-AZ. It is worth to mention here that the amount of azide groups in CNC-AZ (0.15) is approximately two times higher than that of the alkyne groups in CNC-PR (0.073) which in turn means that about 50% of the azide groups can not be engaged in the click reaction. This is in good agreement with the 50% decrease in the azide band intensities in the click reaction products (CNC-click).

Electron micrographs of the click products are shown in Fig. 9. As anticipated, the TEM images of the cross-linked CNCs revealed significantly larger particles being present than those obtained from the initial CNCs or the precursors used (approximately 10 nm in width and about 100–200 nm in length). The particle sizes of the click products were found to vary between 5 and 10 μm length and 2–4 μm width. It is also apparent that the cycloaddition linking reaction has packed the crystals in an organized manner since the rectangular shape of the starting CNCs was retained. Interestingly, the nanoplatelet CNCs prepared in water (Fig. 9(a)) were uniformly oriented, while those prepared in the organic medium DMF (Fig. 9(b)) were an amorphous gel. One possible explanation for the formation of more regular arrays in aqueous media may be the aforementioned self-assembly forces between the hydrated individual CNCs. In accordance with our earlier work, the click chemistry was found to lock into place the CNCs in a uniform vertical arrangement creating the

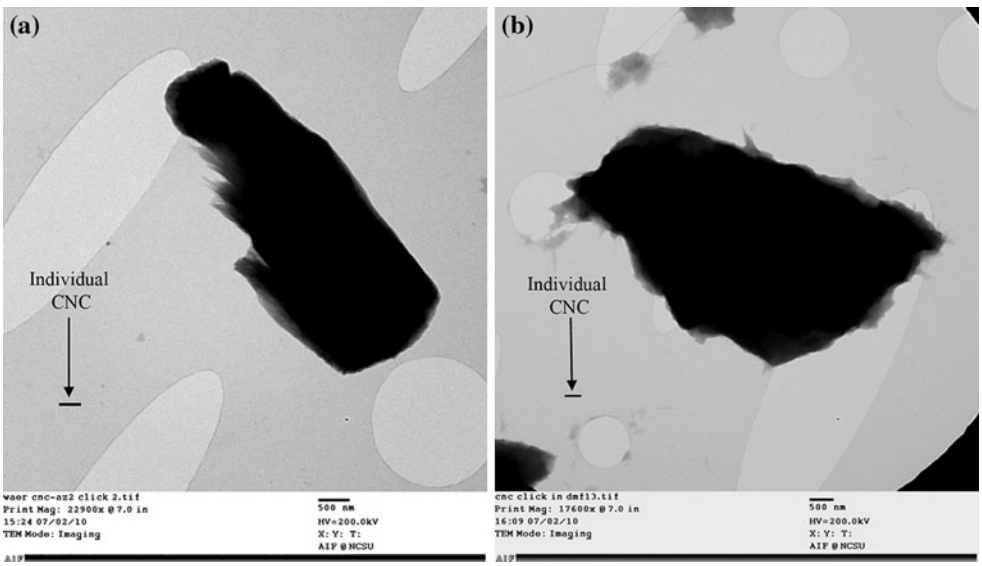

Fig. 9 TEM image of CNC-click product prepared in water (**a**) and DMF (**b**)

observed vertical arrays. However, the blocking of the reducing end groups did not significantly affect the lateral growth of the nanoplatelet CNCs.

Conclusions

Hydrobromic acid (HBr) hydrolysis was used in the production of CNCs. Different reaction parameters were studied and the optimum conditions for the hydrolysis reaction were found to be 2.5 M HBr, 3 h at 100 °C with the concomitant application of sonic energy during the reaction. The produced CNCs were characterized with various methods and found to be highly crystalline with transverse dimensions ranging between 7–8 nm and with lengths of 100–200 nm. The comparison of two separate TEMPO-mediated oxidation methods revealed that the use of acetamino-TEMPO-radical instead of widely employed TEMPO-radical leads to slightly higher degrees of oxidation of the surface hydroxyl groups of CNCs. Furthermore, two important CNC derivatives bearing alkyne and azido functionalities were synthesized and subsequently brought together via click chemistry reaction leading to a formation of regularly packed nanoplatelet cellulose materials. TEM images of the produced materials indicated that the self-assembly forces between the hydrated individual CNCs play a role in controlling the uniformity of the formed nanoplatelet CNCs.

Acknowledgement The authors would like to thank the College of Natural Resources at NCSU for the award of the Hofmann Fellowship to one of us (IF) that made graduate studies possible.

References

1. Battista OA (1950) Ind Eng Chem 42:502
2. Dong X, Revol J, Gray D (1998) Cellulose 5:19
3. Beck-Candanedo S, Roman M, Gray D, Gray G (2005) Biomacromolecules 6:1048
4. Heinze T, Liebert T (2001) Prog Polym Sci 26:1689
5. Klemm DK, Heublein B, Fink HP, Bohn A (2005) Angew Chem Int Ed 44:3358
6. Meldal M, Tornøe CW (2008) Chem Rev 108:2952
7. Helms B, Mynar JL, Hawker CJ, Fréchet JMJ (2004) J Am Chem Soc 126:15020
8. Iha RK, Wooley KL, Nystrom AM, Burke DJ, Kade MJ (2009) Chem Rev 109:5620
9. Liu J, Lam JWY, Tang BZ (2009) Chem Rev 109:5799
10. Binder WH, Sachsenhofer R (2007) Macromol Rapid Commun 28:15
11. Araki J, Wada M, Kuga S, Okano T (1999) J Wood Sci 45:258
12. Araki J, Wada M, Kuga S (2001) Langmuir 17:21
13. Araki J, Wada M, Kuga S, Okano T (1998) Colloids Surf A: Physicochem Eng Aspects 142:75
14. Sipahi-Sağlam E, Gelbrich M, Gruber E (2003) Cellulose 10:237
15. Da Silva Perez D, Montanari S, Vignon MR (2003) Biomacromolecules 4:1417
16. Saito T, Hirota M, Tamura N, Kimura S, Fukuzumi H, Heux L, Isogai A (2009) Biomacromolecules 10:1992
17. Filpponen I, Argyropoulos DS (2010) Biomacromolecules 11:1060
18. Liebert T, Hänsch C, Heinze T (2006) Macromol Rapid Commun 27:208
19. Zhang J, Xu X-D, Wu D-Q, Zhang X-Z, Zhuo. R-X (2009) Carbohydr Polym 77:583
20. Heinze T, Liebert T (2001) Prog Polym Sci 26:1689
21. Xie H, King A, Kilpelainen I, Granstrom M, Argyropoulos DS (2007) Biomacromolecules 8:3740
22. Zoia L, King WT, Argyropoulos DS (2011) J Agric Food Chem 59:829 doi:10.102/JF103615e
23. Dong XM, Kimura T, Revol J, Gray DG (1996) Langmuir 12:2076
24. Segal L, Creely JJ, Martin AE Jr, Conrad CM (1959) Text Res J 29:786
25. Ahtee M, Hattula T, Mangs J, Paakkari T (1999) Paperi Ja Puu 8:475
26. Sugiyama J, Vuong R, Chanzy H (1991) Macromolecules 24:4168
27. Elazzouzi-Hafraoui S, Nishiyama Y, Putaux J-L, Heux L, Dubreuil F, Rochas C (2008) Biomacromolecules 9:57
28. Okita Y, Saito T, Akira Isogai (2010) Biomacromolecules 11:1696
29. Nishiyama Y, Chanzy H, Langan P (2002) J Am Chem Soc 124:9074
30. Tahiri C, Vignon M (2000) Cellulose 7:177
31. Fan LT, Gharpuray MM, Lee Y-H (1987) Biotechnology Monographs. Springer-Verlag, Berlin, p 76
32. Araki J, Wada M, Kuga S, Okano T (2000) Langmuir 16:2413
33. Orts WJ, Godbout L, Marchessault RH, Revol J-F (1998) Macromolecules 31:5717
34. Shibata I, Isogai A (2003) Cellulose 10:151
35. Ibert M, Marsais F, Merbouh N (2002) Carbohydr Res 337:1059
36. Kato Y, Matsuo R, Isogai A (2003) Carbohydr Polym 51:69
37. Beck-Candanedo S, Roman M, Gray DG (2005) Biomacromoleules 6:1048
38. Wang N, Ding E, Cheng R (2008) Langmuir 24:5